International Journal of Engineering & Technology, 7 (4.39) (2018) 94-104

International Journal of Engineering & Technology

Website: www.sciencepubco.com/index.php/IJET

Research paper



Efficient Zigzag Theory for Static and Free Vibration Response of Rectangular FGM Panels

T Das[1]*, J K Nath[2]

[1]*Mechanical Engineering Department, Faculty of Engineering and Technology, Siksha 'O' Anusandhan Deemed to be University, Bhubaneswar, India*

[2]*Mechanical Engineering Department, Faculty of Engineering and Technology, Siksha 'O' Anusandhan Deemed to be University, Bhubaneswar, India*

**Corresponding author E-mail: tapaswineedas@soa.ac.in*

Abstract

An efficient zigzag theory is presented for static and free vibration response of rectangular panels whose layers are made up of a number of functionally graded materials. In order to create a suitable FGM panel laminate, an analytical formulation is developed using an efficient zigzag theory. Different FGM layers have been stacked one over another and perfect interlaminar bonding is assumed between them. As far as manufacturing of such FGM panel is concerned, the technique of 3D printing can be utilized to create it through a single continuous operation. The resulting analytical model is used to identify critical locations and parameters that are responsible for material failure as well as material property variation across panel thickness to enhance productivity and quality of the designed panel. The technique will significantly reduce the time and computational cost involved with analysis of FGM materials and will provide a basis for finite element implementation.

Keywords: *Free vibration; Functionally graded material; FGM panel; Static analysis; Zigzag theory.*

1. Introduction

The men, machines and materials are the three basic inputs in any industry. Not simply the material, it is the smart material that contributes to productivity, sustainability and quality of the product in the emerging era of Industry 4.0. Various segments such as the aerospace industry, automobile industry, health care sectors, sports industry, construction sectors, etc have started using more and more such smart materials. Due to its layered construction or a continuously changing material property from one lateral surface to the other lateral surface, it brings a desired strength and stiffness along with ensuring the basic design parameter of high specific strength and low specific weight. Elasticity as well as inverse elasticity approaches are used for static, free vibration, forced vibration, buckling and transient analysis of such structural laminates manufactured in the form of beams, plates and shells when these laminates are subjected to mechanical loading, thermal loading, thermomechanical loading, electromechanical loading, thermo electromechanical loading, etc.

Smart structures in the form of laminates and continuously graded material properties are more and more used in aeronautical and aerospace industry, automobile industry, civil, marine and other weight sensitive applications due to favourable specific strength, specific stiffness and suitability in highly differing temperature environment. However, the risk of structural failure due to delamination in the layered laminates remains a concern and this occurs due to development of interlaminar transverse shear stress. The functionally graded material (FGM) laminate having a continuous material property variation instead of sharp change at interfaces is a better alternative than the distinct layered laminate construction.

Koizumi [1] first conceived the concept of continuously varying the material properties in a structure and obtained shells and bowls by using silicon carbide and graphite as the two constituent materials. Since then various beam, plate and shell laminates have been designed and analysed for structural application using FGMs. Birman and Byrd [2] have reviewed different models used to calculate effective material properties at any point in the laminate from the material properties of the two constituents. Jha et al. [3] have presented a review concerning the use of FGMs in different applications such as spacecraft, biomedical, mechanical, sensor and thermo-generator applications. Swaminathan et al. [4] and Thai and Kim [5] have reviewed various three dimensional and two dimensional stress and vibration analyses involving FGM plates and shells. Kashtalyan and Menshykova [6] noted reduction in the delamination tendency in sandwich panels when the homogeneous core was replaced by an exponentially varying FG core. Li et al. [7] presented free vibration analysis in FGM sandwich plates by expanding the displacement field through Chebyshev polynomials. Fantuzzi et al. [8] used two dimensional computational models for natural frequencies. A layered approach was adopted in their investigation. Wu and Li [9] adopted a Reissner-type mixed variational theorem based finite layer method by dividing the plate into arbitrary number of layers and used trigonometric functions and Lagrange polynomials to express field variables in each sublayer. First order shear deformation theory has been used by Nguyen et al. [10] for static analysis of FGM plates, by Yang et al. [11] for vibration and damping analysis of viscoelastic and FGM sandwich plates. A discrete stacking approach has been employed by Bernardo et al. [12] in their first order shear deformation theory to study static response and free vibration of FGM plates. The third order theory which gives more accurate results than the first order shear deformation theory has been pre-

Copyright © 2018 Authors. This is an open access article distributed under the Creative Commons Attribution License, which permits unrestricted use, distribution, and reproduction in any medium, provided the original work is properly cited.

sented by Wu and Li [13] by considering interfacial continuity conditions of transverse shear stresses and inplane displacements. Zenkour [14, 15] has presented a number of theories such as sinusoidal, third order, first order and classical theories to analyse symmetric and nonsymmetric FGM sandwich plates. A higher order shear deformation theory was used by Mantari and Soares [16] for bending analysis of FGM sandwich plates. Other generally used theories for FGM laminates are four variable refined plate theory [17, 18, 19] (Thai et al., 2016), five variable generalized shear deformation theory [20, 21], inverse trigonometric shear deformation theory [22], hyperbolic shear deformation theory [23]. A mixed model that uses first order shear deformation theory for face sheets and a three dimensional elasticity solution for weak core is presented by Liu et al. [24] for free vibration analysis of FGM sandwich plates. Carrera et al. [25] have analysed multilayered plates and shells embedding FGM layers inside them. Neves et al. [28, 26, 27] have used meshless technique in higher order shear deformation theory for static and free vibration analysis of FGM sandwich plates. Bending and stress analysis in axisymmetric FGM circular sandwich plates have been performed by Alipour and Shariyat [29] using zigzag theory. They have extended this zigzag theory approach for transient and forced dynamic responses in annular FGM sandwich plates [30].

2. Formulation

A functionally graded material laminate is manufactured by smoothly varying the composition of its constituents from one material to the other material along its transverse direction or axial direction. The geometry of the FGM panel under consideration is shown in Fig.1. The Cartesian coordinate system *xyz* attached to it has the *xy*-plane coinciding with laminate mid-plane. Since the material property at any point in the thickness direction can vary in arbitrary manner, a hypothetical number of layers is devised for the entire laminate and a suitable expression to achieve that arbitrary or desired material distribution is employed in each hypothetical layer. Thus a layered approach is considered to the displacement field approximation. At the same time the continuity conditions on displacements and stresses are needed to be imposed in order to get the realistic variation in these entities as observed from the three dimensional elasticity solutions. In each such hypothetical layer, denoted as k^{th} layer, its bottom and top surfaces are at z_{k-1} and z_k. Thus the laminate with L hypothetical layers has its bottom surface at z_0 and top surface at z_L. The FGM panel has length a along x-axis, infinite width along y-axis and thickness h along z-axis with $z_0 = -h/2$ and $z_L = h/2$.

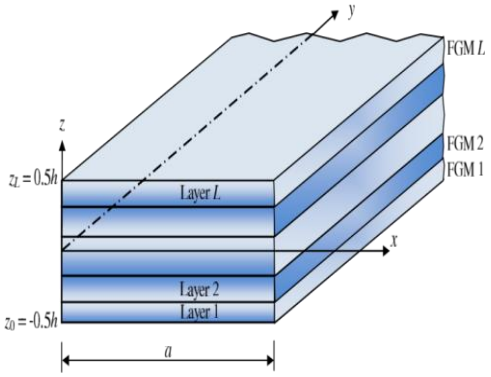


Figure 1: Geometry of FGM panel

Let E_{k_b} and E_{k_t} be the Young's moduli of the bottom and top materials of the kth layer of the panel. Similarly, let the bulk moduli, shear moduli, Poisson's ratios and densities be K_{k_b} and K_{k_t} G_{k_b} and G_{k_t}, and ν_{k_t}, ρ_{k_b} and ρ_{k_t} respectively. With Z_{k-1} and Z_k as the thickness coordinate of the kth layer and power p for volume fraction exponent, the effective values of Young's modulus E_k, Poisson's ratio ν_k and density ρ_k at any point z, such that ($z_{k-1} \le z \le z_k$), in that layer can be expressed by using Voigt's rule of mixtures model (ROM) [31].

$$\begin{aligned} E_k &= E_{k_b} + (E_{k_t} - E_{k_b})V_c \\ \nu_k &= \nu_{k_b} + (\nu_{k_t} - \nu_{k_b})V_c \\ \rho_k &= \rho_{k_b} + (\rho_{k_t} - \rho_{k_b})V_c \end{aligned} \tag{1}$$

where V_c is the volume fraction of the top constituent material and it changes from zero to one from bottom to top of each layer. Present study considers three panel configurations which are shown in Fig.2. Panel A is a symmetric panel for which V_c is expressed as

$$V_c = \begin{Bmatrix} \left(\dfrac{z - z_{k-1}}{z_k - z_{k-1}}\right)^p & bottom\ layer \\ 0 & middle\ layer \\ \left(\dfrac{z - z_k}{z_{k-1} - z_k}\right)^p & top\ layer \end{Bmatrix} \tag{2}$$

For panels B and C, the volume fraction at any point in any hypothetical layer is obtained by using the first line of Eq. (2). It is possible to obtain a pure isotropic layer of top surface material by setting $p = 0$ and a pure isotropic layer of bottom material by setting $p = \infty$.

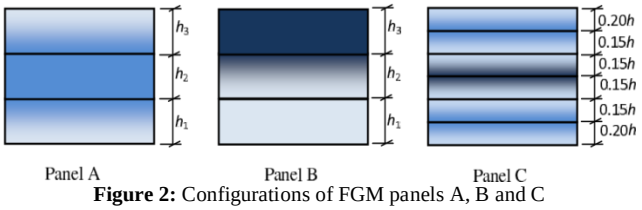


Figure 2: Configurations of FGM panels A, B and C

In order to calculate effective properties in a layer along thickness direction, the Mori-Tanaka model obtains bulk modulus and shear modulus through the constituent properties which are then used for calculation of E_k and ν_k [32].

$$K_k = K_{k_b} + \left(K_{k_t} - K_{k_b}\right)\frac{V_c}{1 + \left(1 - V_c\right)\dfrac{K_{k_t} - K_{k_b}}{K_{k_b} + \dfrac{4}{3}G_{k_b}}}$$

$$G_k = G_{k_b} + \left(G_{k_t} - G_{k_b}\right)\frac{V_c}{1 + \left(1 - V_c\right)\dfrac{G_{k_t} - G_{k_b}}{G_{k_b} + f_1}} \tag{3}$$

$$f_1 = \frac{G_{k_b}\left(9K_{k_b} + 8G_{k_b}\right)}{6\left(K_{k_b} + 2G_{k_b}\right)}$$

$$Y_k = \frac{9K_kG_k}{3K_k + G_k}, \nu_k = \frac{3K_k - 2G_k}{2\left(3K_k + G_k\right)} \tag{4}$$

Assuming negligible transverse normal stress, the constitutive equations for kth layer is

$$\sigma_k = \begin{bmatrix} \sigma_k \\ \tau_{xy} \end{bmatrix}_k = \begin{bmatrix} \bar{Q}_{11} & 0 \\ 0 & \bar{Q}_{66} \end{bmatrix}_k \begin{bmatrix} \varepsilon_x \\ \gamma_{xy} \end{bmatrix}_k = \bar{Q}_k \varepsilon_k \quad (5)$$

$$\tau_k = \begin{bmatrix} \tau_{zx} \\ \tau_{yz} \end{bmatrix}_k = \begin{bmatrix} \bar{Q}_{55} & 0 \\ 0 & \bar{Q}_{44} \end{bmatrix}_k \begin{bmatrix} \gamma_{zx} \\ \gamma_{yz} \end{bmatrix}_k = \hat{Q}_k \gamma_k \quad (6)$$

where the reduced stiffnesses Q_{ij} are related to engineering constants by

$$Q_{11_k} = \frac{Y_k}{1 - v_k^2}, Q_{44_k} = Q_{55_k} = Q_{66_k} = \frac{Y_k}{2(1+v_k)} \quad (7)$$

The displacement field is assumed to be

$$u(x,z,t) = u_k(x,t) = zw_{0_d} + z\psi_k(x,t) + z^2\xi(x,t) + z^3\eta(x,t) \quad (8)$$

$$w(x,z,t) = w_0(x,t) \quad (9)$$

With

$$u_k = \begin{bmatrix} u_{k_x} \\ u_{k_y} \end{bmatrix}, w_{0_d} = \begin{bmatrix} w_{0,x} \\ 0 \end{bmatrix}, \psi_k = \begin{bmatrix} \psi_{k_x} \\ \psi_{k_y} \end{bmatrix}, \xi = \begin{bmatrix} \xi_x \\ \xi_y \end{bmatrix}, \eta = \begin{bmatrix} \eta_x \\ \eta_y \end{bmatrix} \quad (10)$$

Since the FGM panel is infinitely long in the *y*-direction, the derivative of any quantity with respect to *y* is zero. Thus the non-zero strains become $\varepsilon_x = u_{x,x}$, $\gamma_{xy} = u_{y,x}$, $\gamma_{yz} = u_{y,z}$, $\gamma_{zx} = u_{x,z} + w_{,x}$. These strains can be expressed in terms of displacements given in Eqs.(8) and (9) and then the stress-strain relation in Eq.(6) can be used to obtain transverse shear stress as

$$\tau = \hat{Q}^k \left[\psi_k + 2z\xi + 3z^2\eta \right] \quad (11)$$

Each FGM layer in the FGM laminate can be distinct and of different material constituents resulting in material property discontinuity at the interfaces. This will result in discontinuity of inplane displacements and transverse shear stresses. However, the continuity condition for these entities can be imposed to yield their smooth variation and also it will lead to elimination of their layer dependency. The transversely loaded FGM panel has zero shear taction on its top and bottom surfaces. Utilization of these conditions leads to

$$u(x,z,t) = u_0(x,t) - zw_{0d} + R^k(z)\psi_0(x,t) \quad (12)$$

where $R^k(z)$ contains the contribution of global as well as local coefficients. The equations of motion as well as boundary conditions are derived using Hamilton's principle. The equations of motion expressed in terms of stress resultants are

$$I_{11}\ddot{u}_{0_x} - I_{13}\ddot{w}_{0,x} + I_{15}\ddot{\psi}_{0_x} - N_{x,x} = 0 \quad (13)$$

$$I_{22}\ddot{u}_{0y} - I_{26}\ddot{\psi}_{0y} - N_{xy,x} = 0 \quad (14)$$

$$I_{13}\ddot{u}_{0_x,x} - I_{33}\ddot{w}_{0,xx} + I_{35}\ddot{\psi}_{0_x,x} + I_{33}\ddot{w}_0 - M_{x,xx} + N_x - p_z^1 - p_z^2 = 0 \quad (15)$$

$$I_{15}\ddot{u}_{0_x} - I_{35}\ddot{w}_{0,x} + I_{55}\ddot{\psi}_{0_x} - P_{x,x} + Q_x = 0 \quad (16)$$

$$I_{26}\ddot{u}_{0_y} + I_{66}\ddot{\psi}_{0_y} = P_{xy,x} + Q_y = 0 \quad (17)$$

I_{11}, I_{13}, I_{15}, I_{22}, I_{26}, I_{33}, I_{35}, I_{55}, I_{66} are non-zero coefficient of inertia matrix I having expressions.

$$\begin{bmatrix} I_{11} & 0 \\ 0 & I_{22} \end{bmatrix}, \begin{bmatrix} I_{13} \\ 0 \end{bmatrix}, \begin{bmatrix} I_{15} & 0 \\ 0 & I_{26} \end{bmatrix} = \left\langle \rho I_2, I_1 \rho z, \rho R^k \right\rangle \quad (18)$$

$$\begin{bmatrix} I_{33} \\ 0 \end{bmatrix}, \begin{bmatrix} I_{35} \\ 0 \end{bmatrix}, \begin{bmatrix} I_{55} & 0 \\ 0 & I_{66} \end{bmatrix} = \left\langle I_1 \rho z^2, I_1 \rho z R^k, \rho R^{kT} R^k \right\rangle, \bar{I}_{33} = 0 \quad (19)$$

and the notation <···> stands for integration across the thickness and is given by $\langle ... \rangle = \sum_{k=1}^{L} \int_{z_{k-1}}^{z_k} (...) dz$. The stress and moment resultants N_x, N_{xy}, M_x, P_x, P_{xy}, Q_x, Q_y are given by

$$N_x = \langle \sigma_x \rangle, N_{xy} = \langle \tau_{xy} \rangle, M_x = \langle z\sigma_x \rangle, P_x = \langle R_{11}^k \sigma_k \rangle$$
$$P_{xy} = \langle P_{11}^k \tau_{xy} \rangle, Q_x = \langle R_{11,z}^k \tau_{zx} \rangle, Q = \langle R_{22,z}^k \tau_{yz} \rangle$$

The boundary conditions at edges at x = 0, a are any one value of each of following product:

$$u_{0_x} N_x, u_{0_y} N_{xy}, w_0 M_{x,x}, w_{0,x} M_x, \psi_{0_x} P_x, \psi_{0_y} P_{xy} \quad (20)$$

The stress resultants are now expressed in terms of displacement variables and substituted in Eqs. (13)–(17) to yield equations of motion involving displacement variables:

$$\bar{L}\ddot{U} + LU = \bar{P} \quad (21)$$

$$U = \left[u_{0_x} u_{0_y} w_0 \psi_{0_x} \psi_{0_y} \right]^T, P = \left[0\ 0\ -\left(p_z^1 + p_z^2 \right)\ 0\ 0 \right]^T \quad (22)$$

and $\bar{L}$ and L being differential operators in *x* and *y*. In order to obtain analytical solution for simply supported FGM panel that has following prescribed values at its boundaries at *x = 0, a*

$$u_{0_x} = 0, N_y = 0, w_0 = 0, M_y = 0, \psi_{0_x} = 0, P_y = 0 \quad (23)$$

Fourier series is used to expand the variables as

$$\left(u_{0_x}, \psi_{0_x} \right) = \sum_{m=1}^{\infty} \left(u_{0_x}, \psi_{0_x} \right)_m \cos \frac{m\pi x}{a} \quad (24)$$

$$\left(u_{0_y}, \psi_{0_y}, w_0 \right) = \sum_{m=1}^{\infty} \left(u_{0_y}, \psi_{0_y}, w_0 \right)_m \sin \frac{m\pi x}{a} \quad (25)$$

Actually the Fourier expansion is truncated after a number of terms at which the results show convergence. In sinusoidally loaded case, only one term is taken and in uniform loading the number of terms is decided based on a convergence study. These expansions are now substituted in Eq. (21) and the equation involving mass matrix *M* and stiffness matrix *K* is obtained as

$$M\ddot{U}^m + KU^m = \bar{P}^m \quad (26)$$

Cylindrical bending response under statically applied load is obtained by dropping the term involving *M* in Eq. (26) and inverting the resulting expression. The displacement entities are then substituted in strain displacement relations and stress strain relations to obtain the strains and stresses. In the present study, the inplane stresses are obtained from constitutive relations while the transverse shear stresses are obtained by integrating the three dimensional equilibrium equations. The free vibration response is obtained by setting the loading term to zero in the right side of Eq. (26). The eigen values of the resulting expression denote the square of the natural frequencies and the associated eigenvector denote the corresponding mode shapes.

3. Results and Discussion

As shown in Fig. 2 three FGM panels are taken up for static and free vibration analysis. Cylindrical bending response is investigated under sinusoidal as well as uniform loads. First five natural frequencies have been analyzed for free vibration response. Three constituent materials, viz, aluminium, zirconia and alumina are used of which aluminium is micro-mechanically mixed with zirconia or alumina in a continuously varying manner to form a FGM layer using rule of mixtures model as well as Mori-Tanaka model. The material properties of these isotropic constituents are given in Table 1.

Table 1: Material properties

Material	*E* (GPa)	*v*	ρ (kg/m^3)
Aluminium	70.0	0.3	2702
Zirconia	151.0	0.3	3000
Alumina	380.0	0.3	3800

3.1. Cylindrical Bending Under Sinusoidal Load

Exact three dimensional elasticity solution for multilayered FGM plates or panels are not available in the literature, but such solution is available for a single layer FGM plate [33]. The present formulation is validated for such a square FGM plate under sinusoidal load on the top surface. The validation is shown in Table 2 for three aspect ratios of $S = a/h$ = 4,10,50 by noting the magnitudes at typical locations along with their percent errors within parentheses. The table shows that the present formulation is very much accurate even for a thick panel with aspect ratio S = 4.

Response to sinusoidal load of $p_0 \sin(\pi x/a)$ applied on top surface of the panel is obtained for displacements u, w and stresses σ_x, τ_{zx} in the following non-dimensionalized form with E_0 = 1 GPa.

$$(\bar{u},\bar{w}) = 100(u, w/S)E_0/p_0 hS^3, (\bar{\sigma}_x, \bar{\tau}_{zx}) = (\sigma_x, S\tau_{zx})/P_0 S^2 \qquad (27)$$

Non-dimensionalized results obtained for three layered symmetric FGM panel A are shown in Table 3 for four sets of thickness ratios. Its bottom FGM layer changes from aluminium to zirconia, middle layer remains fully of zirconia and top FGM layer changes from zirconia to aluminium. The volume fraction of the bottom and top FGM layers changes in the same fashion as we move away from the mid-plane of the panel in both directions. Thus it is a completely symmetric panel. The thickness ratios h_1:h_2:h_3 are 2:1:2, 1:1:1, and 1:2:1, 1:2:1, 1:8:1. Three values of the power *p* of volume fraction exponent is taken at 1, 4 and 10 and for each value of *p* three values of aspect ratio *S* at 5, 10 and 20 are considered. The reported location is included within parenthesis alongside the respective entity. Both displacement components $\bar{u}$ and $\bar{w}$ are seen to decrease as the FGM panel becomes thinner at a given power index *p*. At the same time, the displacements get increased with increase of power index at a given aspect ratio. This shows that a thin panel is less stiff than a thick panel. With increase of the power index the outside constituent materials (aluminium) of the two FGM layers dominate their presence, thereby making the entire panel less stiff with consequent high displacements. However, as we increase the thickness of the stiffer mid layer by changing the thickness ratios from 2:1:2 to 1:8:1 through 1:1:1 and 1:2:1, we see the decrease in the displacements that indicate the increase of the panel stiffness. Both the rule of mixtures model (ROM) and the Mori-Tanaka model (MTM) show the same observations. Kapuria et al.[32] have established that the Mori-Tanaka model capable of predicting close interactions between the constituent materials yields much accurate results than the simple yet widely used rule of mixtures model. The Young's modulus predicted by MTM is significantly lower than the ROM and hence the displacements obtained using MTM is more than that using ROM. Table 4 shows response entities for non-symmetric panel B for same set of thickness ratios. Bottom layer of this panel B is entirely of aluminium, its middle layer changes from aluminium to alumina and the top layer is fully alumina. Its top is thus stiffer than its bottom. The ceramic constituent of this panel is stiffer than that of panel A and owing to the presence towards the top surface the resulting displacements are smaller than that of panel A. As expected the transverse shear stress has increased in the case of narrow middle layer panel and the reverse is observed steadily with increase of middle layer thickness. For any given aspect ratio increase in value of the power law index makes that layer rich with the presence of the second constituent material. This implies the panel becomes more stiff and hence induces less transverse shear stress at the center of the panel.

Through-thickness distribution of $\bar{u},\bar{w},\bar{\sigma}_x$ and $\bar{\tau}_{zx}$ obtained in panels A and B under this sinusoidal loading using Mori-Tanaka model are shown in Figs.3–5 with layer thickness ratios 2:1:2, 1:2:1 and 1:8:1 respectively. The displacement distribution in Fig.3 with 2:1:2 thickness ratio and in Fig.4 with 1:2:1 thickness ratio indicate that the local stiffness at every point in the non-symmetric panel B has increased. But it can be seen from displacement distribution in Fig.5 that significantly increasing the middle layer thickness has made the non-symmetric panel B less stiff at every point in spite of the presence of a stiffer ceramic constituent in it. Thus it is not only the presence of a stiff material that makes a panel stiff, rather the combination of layer thickness and material type along with the distribution of its constituents decides whether it will be locally less stiff or more stiff. A non-linear pattern of inplane normal stress is observed in the symmetric panel A in its two outer FGM layers and this has turned highly non-linear with decrease in thickness of these FGM layers. A smoother variation of this inplane normal stress is observed in non-symmetric panel B with decrease of thickness in its two outer layers. Whereas the distribution symmetry of the constituent materials has not significantly altered the magnitude and location of the transverse shear stress in panel A, the non-symmetric distribution of constituent materials has lowered the magnitude as well as shifted its location towards the middle of the FGM layer with increase in its thickness in panel B.

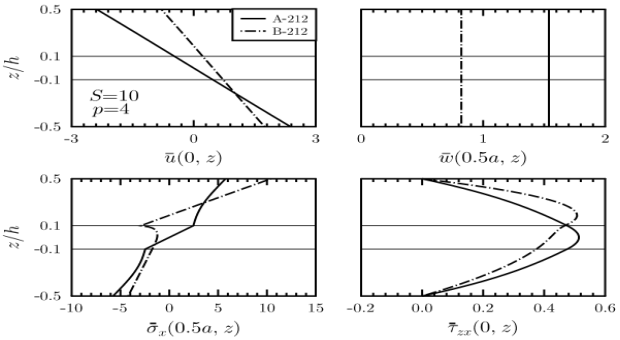


Figure 3: Through-thickness distributions of response entities in FGM panels A and B under sinusoidal loading with Mori-Tanaka model

Table 2: Validation with 3D exact solution for square FGM plate under sinusoidal load on top

Entity	*S*=4		*S*=10		*S*=50	
	3D [33]	Present	3D [33]	Present	3D [33]	Present
$\bar{u}(-0.5h)$	-0.004069	-0.0041800	-0.02472	-0.024802	-0.6141	-0.61398
		(2.73%)		(0.33%)		(-0.02%)
$\bar{w}(0)$	-0.01370	-0.014205	-0.1707	-0.17179	-20.33	-20.322
		(3.69%)		(0.64%)		(-0.04%)
$\bar{\sigma}_x(-0.5h)$	3.631	3.7301	22.06	22.133	548.0	547.90
		(2.73%)		(0.33%)		(-0.02%)
$\bar{\tau}_{xz}(0)$	-0.9500	-0.94496	-2.396	-2.3936	-12.00	-11.997
		(-0.53%)		(-0.10%)		(-0.03%)
$\bar{\sigma}_z(0)$	-0.5130	-0.51451	-0.5142	-0.51415	-0.5141	-0.51409
		(0.29%)		(-0.01%)		(0.00%)

Table 3: Displacements and transverse shear stress in FGM panel A under sinusoidal load on top

p	*S*	ROM			Mori-Tanaka		
		$\bar{u}(-0.5h)$	$\bar{w}(0)$	$\bar{\tau}_{xz}(0)$	$\bar{u}(-0.5h)$	$\bar{w}(0)$	$\bar{\tau}_{xz}(0)$
2-1-2 thickness ratio							
1 5	5	1.8765	1.2738	0.51666	1.9909	1.3488	0.51780
	10	1.8554	1.2010	0.51812	1.9693	1.2741	0.51926
	20	1.8501	1.1828	0.51848	1.9639	1.2554	0.51962
4	5	2.3640	1.5950	0.51612	2.4035	1.6224	0.51221
	10	2.3412	1.5130	0.51759	2.3804	1.5385	0.51367
	20	2.3355	1.4924	0.51795	2.3746	1.5175	0.51403
10	5	2.4783	1.6749	0.50478	2.4900	1.6838	0.50237
	10	2.4546	1.5870	0.50624	2.4660	1.5946	0.50383
	20	2.4487	1.5650	0.50660	2.4600	1.5723	0.50419
1-1-1 thickness ratio							
1	5	1.7884	1.2148	0.51850	1.8924	1.2824	0.52180
	10	1.7678	1.1445	0.51995	1.8715	1.2108	0.52324
	20	1.7627	1.1269	0.52032	1.8662	1.1929	0.52361
4	5	2.2390	1.5081	0.52892	2.2837	1.5377	0.52702
	10	2.2172	1.4322	0.53039	2.2617	1.4608	0.52849
	20	2.2117	1.4132	0.53075	2.2562	1.4416	0.52886
10	5	2.3691	1.5946	0.52340	2.3856	1.6059	0.52178
	10	2.3470	1.5158	0.52488	2.3635	1.5264	0.52326
	20	2.3415	1.4960	0.52525	2.3579	1.5065	0.52363
1-2-1 thickness ratio							
1	5	1.6578	1.1292	0.51659	1.7409	1.1828	0.52151
	10	1.6377	1.0610	0.51803	1.7204	1.1139	0.52295
	20	1.6326	1.0440	0.51839	1.7153	1.0966	0.52331
4	5	2.0181	1.3618	0.53590	2.0601	1.3890	0.53651
	10	1.9966	1.2903	0.53733	2.0386	1.3172	0.53795
	20	1.9912	1.2725	0.53768	2.0332	1.2992	0.53831
10	5	2.1407	1.4414	0.53769	2.1591	1.4534	0.53750
	10	2.1191	1.3687	0.53914	2.1375	1.3805	0.53895
	20	2.1137	1.3505	0.53951	2.1321	1.3623	0.53932
1-8-1 thickness ratio							
1	5	1.3818	0.95092	0.49794	1.4144	0.97185	0.50141
	10	1.3631	0.88561	0.49942	1.3953	0.90617	0.50287
	20	1.3584	0.86927	0.49979	1.3906	0.88974	0.50323
4	5	1.5161	1.0373	0.51200	1.5335	1.0485	0.51362
	10	1.4961	0.97048	0.51339	1.5134	0.98156	0.51500
	20	1.4911	0.95377	0.51374	1.5084	0.96480	0.51535
10	5	1.5661	1.0695	0.51664	1.5747	1.0750	0.51739
	10	1.5458	1.0022	0.51801	1.5543	1.0076	0.51876
	20	1.5407	0.98538	0.51835	1.5492	0.99077	0.51910

Table 4: Displacements and transverse shear stress in FGM panel B under sinusoidal load on top

p	S	ROM			Mori-Tanaka		
		$\bar{u}(-0.5h)$	$\bar{w}(0)$	$\bar{\tau}_{xz}(0.2h)$	$\bar{u}(-0.5h)$	$\bar{w}(0)$	$\bar{\tau}_{xz}(0.2h)$
2-1-2 thickness ratio							
1	5	1.6155	0.81626	0.53328	1.6824	0.84277	0.52180
	10	1.6073	0.77589	0.53328	1.6736	0.79847	0.52179
	20	1.6053	0.76579	0.53328	1.6714	0.78739	0.52178
4	5	1.7278	0.86123	0.51390	1.7517	0.87130	0.50722
	10	1.7186	0.81388	0.51387	1.7420	0.82140	0.50720
	20	1.7163	0.80203	0.51386	1.7396	0.80890	0.50720
10	5	1.7587	0.87431	0.50554	1.7680	0.87850	0.50249
	10	1.7489	0.82369	0.50552	1.7579	0.82650	0.50249
	20	1.7464	0.81102	0.50551	1.7553	0.81348	0.50249
1-1-1 thickness ratio							
1	5	1.5672	0.79795	0.53191	1.6762	0.84220	0.51502
	10	1.5586	0.75728	0.53197	1.6665	0.79473	0.51512
	20	1.5564	0.74709	0.53198	1.6641	0.78285	0.51515
4	5	1.7563	0.87559	0.50166	1.7864	0.89029	0.49128
	10	1.7456	0.82220	0.50179	1.7744	0.83153	0.49155
	20	1.7430	0.80883	0.50182	1.7714	0.81681	0.49161
10	5	1.7972	0.89542	0.48817	1.8057	0.90105	0.48395
	10	1.7849	0.83501	0.48846	1.7926	0.83759	0.48436
	20	1.7818	0.81988	0.48853	1.7894	0.82169	0.48447
1-2-1 thickness ratio							
1	5	1.4817	0.76575	0.52923	1.6419	0.83348	0.51091
	10	1.4723	0.72458	0.52935	1.6307	0.78202	0.51121
	20	1.4699	0.71427	0.52938	1.6279	0.76913	0.51128
4	5	1.7695	0.88893	0.49303	1.8002	0.91002	0.48222
	10	1.7566	0.82697	0.49348	1.7846	0.83798	0.48297
	20	1.7533	0.81146	0.49360	0.1781	0.81994	0.48316
10	5	1.8140	0.91812	0.47803	1.8179	0.92677	0.47537
	10	1.7976	0.84249	0.47892	1.7998	0.84528	0.47637
	20	1.7935	0.82354	0.47914	1.7953	0.82487	0.47662
1-8-1 thickness ratio							
1	5	1.2900	0.69489	0.51026	1.5480	0.81536	0.49565
	10	1.2793	0.65298	0.51030	1.5346	0.75822	0.49585
	20	1.2766	0.64249	0.51031	1.5313	0.74392	0.49590
4	5	1.7758	0.92259	0.47848	1.8164	0.97314	0.46293
	10	1.7590	0.84586	0.47888	1.7950	0.87824	0.46334
	20	1.7548	0.82665	0.47898	1.7897	0.85447	0.46344
10	5	1.8296	0.98776	0.45915	1.8442	1.0225	0.45122
	10	1.8060	0.88412	0.45965	1.8185	0.91063	0.45155
	20	1.8001	0.85816	0.45978	1.8121	0.88261	0.45163

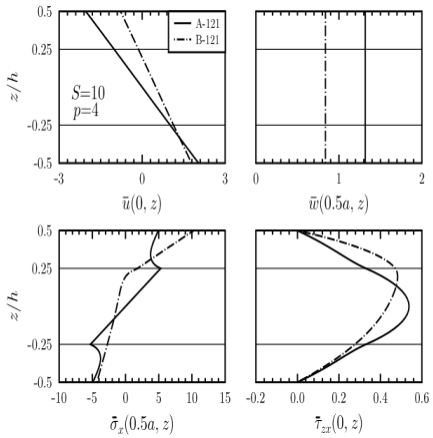


Figure 4: Through-thickness distributions of response entities in FGM panels A and B under sinusoidal loading with Mori-Tanaka model

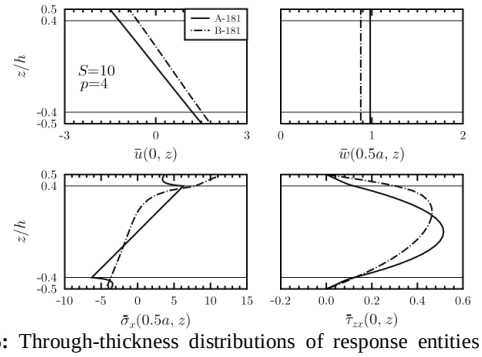


Figure 5: Through-thickness distributions of response entities in FGM panels A and B under sinusoidal loading with Mori-Tanaka model

Table 5 compares the magnitudes of the response entities at typical locations using both rule of mixtures model and Mori-Tanaka model obtained for the six layer FGM panel C whereas the

through-thickness distributions are shown in Fig.6 obtained using MoriTanaka model. Table 5 establishes the panel C becoming less stiff with increase in the power law index *p*. Increasing the value of *p* also increases non-linearity in the inplane normal stress profile and increases smoothness in the transverse shear stress distribution profile. The effect of power law index *p* on the variation of the displacements and stresses is shown in Figs. 7 and 8 using rule of mixtures and Mori-Tanaka model respectively in the three thick FGM panels with aspect ratio S = 5. The response entities attain saturation at p = 20.

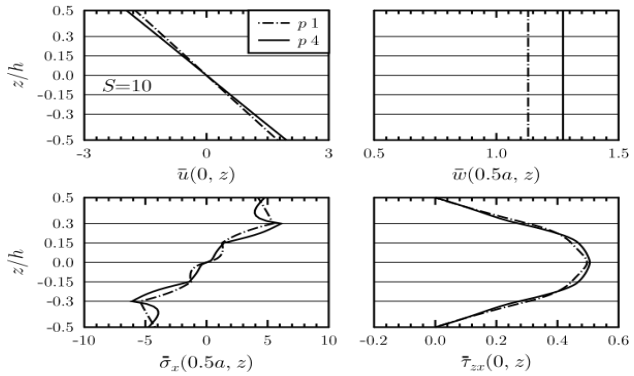


Figure 6: Through-thickness distributions of response entities in FGM panel C under sinusoidal loading with Mori-Tanaka model

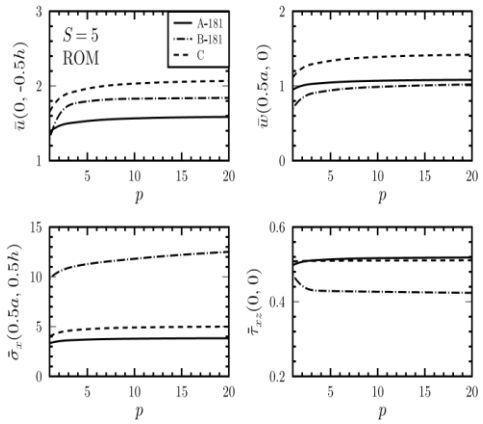


Figure 7: Effect of power law index in FGM panels A, B and C under sinusoidal loading with ROM

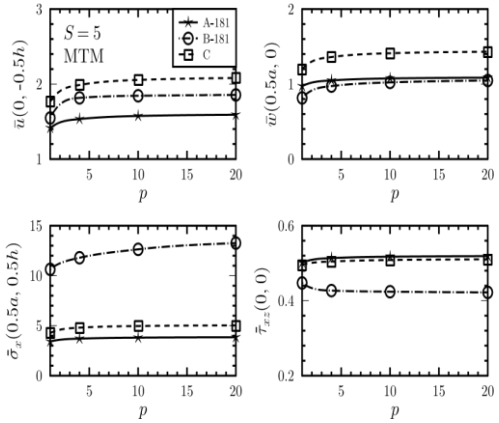


Figure 8: Effect of power law index in FGM panels A, B and C under sinusoidal loading with MTM

3.2. Cylindrical Bending Under Uniform Load

A uniform pressure load $p_z^2 = -p_0$ is applied on the top surface of the FGM panel. In order to determine the number of terms *m* in the Fourier series expansion a convergence check is conducted and found that (m = 301) provide convergence to all displacements and stresses. Taking (m = 301) the results for displacements and stresses are obtained and shown in Table 6 for panel A, in Table 7 for panel B and in Table 8 for panel C. Both ROM and Mori-Tanaka models are used in obtaining effective material properties at any point across the panel thickness. As done for sinusoidal loading case four layer thickness ratios are considered for panels A and B. The increasing or decreasing tendency as observed in sinusoidal loading case is here observed for all FGM panels. The magnitude of displacements are more since the average value of uniform load is more than that of sinusoidal load. The corresponding resulting stresses under uniform loading are also higher than that induced under sinusoidal loading. The symmetric and non-symmetric material property distribution has significant influence on the displacement and stress profiles which are shown in Figs.9–11 for all FGM panels A and B with layer thickness ratios 2:1:2, 1:2:1 and 1:8:1 at S = 10 and p = 4. The through-thickness distributions are given in Fig.12 for moderately thick (S = 10) FGM panel C with two values of power law index at p = 1 and 4. It is observed that higher magnitudes are associated at typical locations with higher values of power law index.

Table 5: Displacements and transverse shear stress in FGM panel C under sinusoidal load on top

p	S	ROM			Mori-Tanaka		
		$\bar{u}(-0.5h)$	$\bar{w}(0)$	$\bar{\tau}_{xz}(0.2h)$	$\bar{u}(-0.5h)$	$\bar{w}(0)$	$\bar{\tau}_{xz}(0.2h)$
1	5	1.6526	1.1136	0.50795	1.7654	1.1993	0.49566
	10	1.6365	1.0572	0.50915	1.7459	1.1303	0.49689
	20	1.6325	1.0431	0.50945	1.7410	1.1131	0.49720
4	5	1.9354	1.3152	0.50951	1.9881	1.3607	0.50457
	10	1.9126	1.2384	0.51077	1.9622	1.2730	0.50593
	20	1.9069	1.2192	0.51109	1.9558	1.2510	0.50627
10	5	2.0318	1.3891	0.51025	2.0553	1.4114	0.50850
	10	2.0056	1.3007	0.51164	2.0271	1.3163	0.50998
	20	1.9990	1.2786	0.51199	2.0201	1.2925	0.51035

Table 6: Displacements and stresses in FGM panel A under uniform load on top

p	S	ROM				Mori-Tanaka			
		$\bar{u}(-0.5h)$	$\bar{w}(0)$	$\bar{\sigma}_x(0.5h)$	$\bar{\tau}_{xz}(0)$	$\bar{u}(-0.5h)$	$\bar{w}(0)$	$\bar{\sigma}_x(0.5h)$	$\bar{\tau}_{xz}(0)$
2-1-2 thickness ratio									
1	5	2.4313	1.6123	5.5787	0.75612	2.5792	1.7074	5.9193	0.75767
	10	2.3989	1.5224	5.5276	0.78683	2.5461	1.6151	5.8672	0.78852
	20	2.3907	1.4999	5.5148	0.80204	2.5377	1.5920	5.8541	0.80380

4	5	3.0617	2.0193	7.0309	0.75392	3.1128	2.0539	7.1483	0.74789
	10	3.0266	1.9180	6.9756	0.78540	3.0773	1.9504	7.0924	0.77930
	20	3.0178	1.8927	6.9618	0.80099	3.0683	1.9244	7.0784	0.79486
10	5	3.2097	2.1203	7.3711	0.73634	3.2248	2.1316	7.4055	0.73283
	10	3.1733	2.0118	7.3137	0.76770	3.1880	2.0215	7.3475	0.76404
	20	3.1641	1.9847	7.2994	0.78323	3.1787	1.9939	7.3330	0.77949
1-1-1 thickness ratio									
1	5	2.3174	1.5376	5.3165	0.75919	2.4518	1.6233	5.6263	0.76407
	10	2.2857	1.4508	5.2666	0.78979	2.4196	1.5349	5.5756	0.79483
	20	2.2777	1.4291	5.2542	0.80495	2.4115	1.5128	5.5629	0.81008
4	5	2.9000	1.9093	6.6590	0.77391	2.9576	1.9469	6.7920	0.77066
	10	2.8663	1.8156	6.6060	0.80544	2.9239	1.8520	6.7389	0.80234
	20	2.8578	1.7922	6.5928	0.82105	2.9154	1.8282	6.7256	0.81803
10	5	3.0680	2.0189	7.0466	0.76437	3.0894	2.0332	7.0958	0.76178
	10	3.0341	1.9216	6.9931	0.79639	3.0554	1.9351	7.0422	0.79383
	20	3.0255	1.8973	6.9797	0.81225	3.0468	1.9106	7.0288	0.80970
1-2-1 thickness ratio									
1	5	2.1485	1.4291	4.9275	0.75680	2.2559	1.4971	5.1749	0.76445
	10	2.1175	1.3450	4.8788	0.78705	2.2244	1.4120	5.1253	0.79475
	20	2.1097	1.3240	4.8666	0.80204	2.2165	1.3907	5.1129	0.80976
4	5	2.6144	1.7239	6.0005	0.78653	2.6687	1.7585	6.1258	0.78720
	10	2.5814	1.6358	5.9486	0.81711	2.6356	1.6699	6.0738	0.81794
	20	2.5730	1.6137	5.9356	0.83226	2.6273	1.6477	6.0607	0.83317
10	5	2.7728	1.8248	6.3659	0.78848	2.7965	1.8401	6.4208	0.78799
	10	2.7396	1.7352	6.3137	0.81955	2.7634	1.7501	6.3686	0.81916
	20	2.7312	1.7127	6.3007	0.83494	2.7550	1.7276	6.3555	0.83460
1-8-1 thickness ratio									
1	5	1.7914	1.2031	4.1057	0.72762	1.8336	1.2296	4.2025	0.73322
	10	1.7627	1.1225	4.0605	0.75782	1.8043	1.1486	4.1564	0.76333
	20	1.7554	1.1023	4.0491	0.77279	1.7970	1.1283	4.1449	0.77826
4	5	1.9653	1.3126	4.5049	0.75036	1.9879	1.3268	4.5570	0.75299
	10	1.9346	1.2301	4.4566	0.78019	1.9570	1.2442	4.5084	0.78277
	20	1.9268	1.2095	4.4445	0.79497	1.9492	1.2235	4.4962	0.79752
10	5	2.0301	1.3534	4.6540	0.75790	2.0411	1.3603	4.6794	0.75912
	10	1.9989	1.2704	4.6048	0.78759	2.0098	1.2772	4.6300	0.78879
	20	1.9910	1.2496	4.5925	0.80229	2.0019	1.2564	4.6177	0.80348

Table 7: Displacements and stresses in FGM panel B under uniform load on top

p	*S*	ROM				Mori-Tanaka			
		$\bar{u}(-0.5h)$	$\bar{w}(0)$	$\bar{\sigma}_x(0.5h)$	$\bar{\tau}_{xz}(0)$	$\bar{u}(-0.5h)$	$\bar{w}(0)$	$\bar{\sigma}_x(0.5h)$	$\bar{\tau}_{xz}(0)$
2-1-2 thickness ratio									
1	5	2.0897	1.0335	12.984	0.61097	2.1763	1.0669	13.014	0.60329
	10	2.0773	0.98363	12.843	0.63867	2.1630	1.0122	12.859	0.63112
	20	2.0741	0.97117	12.807	0.65243	2.1596	0.99855	12.820	0.64496
4	5	2.2352	1.0902	13.035	0.59853	2.2662	1.1028	13.009	0.60599
	10	2.2211	1.0317	12.869	0.62661	2.2514	1.0412	12.835	0.63456
	20	2.2176	1.0171	12.827	0.64058	2.2476	1.0258	12.791	0.64877
10	5	2.2753	1.1066	13.007	0.60768	2.2875	1.1119	12.988	0.61152
	10	2.2603	1.0442	12.830	0.63643	2.2719	1.0477	12.806	0.64043
	20	2.2564	1.0285	12.785	0.65073	2.2680	1.0316	12.761	0.65482
1-1-1 thickness ratio									
1	5	2.0275	1.0102	12.826	0.63775	2.1687	1.0660	12.904	0.62243
	10	2.0143	0.96002	12.683	0.66666	2.1538	1.0075	12.739	0.65097
	20	2.0110	0.94746	12.648	0.68103	2.1501	0.99279	12.698	0.66517
4	5	2.2724	1.1081	12.951	0.61298	2.3117	1.1265	12.899	0.62164
	10	2.2562	1.0422	12.766	0.64157	2.2935	1.0540	12.696	0.65051
	20	2.2520	1.0257	12.719	0.65580	2.2888	1.0358	12.645	0.66488
10	5	2.3257	1.1330	12.888	0.62408	2.3371	1.1399	12.858	0.62783
	10	2.3070	1.0584	12.679	0.65315	2.3171	1.0616	12.640	0.65685

	20	2.3022	1.0397	12.627	0.66762	2.3120	1.0420	12.586	0.67131
1-2-1 thickness ratio									
1	5	1.9173	0.96935	12.557	0.66358	2.1248	1.0548	12.791	0.63763
	10	1.9029	0.91854	12.413	0.69347	2.1077	0.99127	12.615	0.66665
	20	1.8992	0.90583	12.378	0.70833	2.1034	0.97538	12.571	0.68109
4	5	2.2902	1.1246	12.917	0.62146	2.3306	1.1509	12.903	0.62758
	10	2.2705	1.0482	12.707	0.65019	2.3070	1.0620	12.664	0.65620
	20	2.2655	1.0290	12.654	0.66450	2.3009	1.0398	12.604	0.67046
10	5	2.3487	1.1611	12.881	0.63031	2.3543	1.1718	12.915	0.63139
	10	2.3237	1.0677	12.631	0.65899	2.3268	1.0712	12.651	0.65978
	20	2.3174	1.0443	12.569	0.67328	2.3198	1.0460	12.585	0.67394
1-8-1 thickness ratio									
1	5	1.6700	0.87945	12.036	0.68782	2.0042	1.0316	13.065	0.64866
	10	1.6537	0.82772	11.891	0.71834	1.9838	0.96103	12.879	0.67862
	20	1.6495	0.81477	11.855	0.73352	1.9786	0.94338	12.833	0.69353
4	5	2.2996	1.1667	13.646	0.62086	2.3534	1.2300	14.471	0.61715
	10	2.2740	1.0720	13.407	0.65051	2.3209	1.1128	14.198	0.64697
	20	2.2675	1.0483	13.347	0.66528	2.3126	1.0835	14.130	0.66183
10	5	2.3712	1.2481	14.481	0.61709	2.3907	1.2918	15.502	0.61225
	10	2.3352	1.1202	14.189	0.64666	2.3516	1.1537	15.207	0.64221
	20	2.3261	1.0882	14.116	0.66140	2.3416	1.1191	15.133	0.65714

Table 8: Displacements and stresses in FGM panel C under uniform load on top

p	S	ROM				Mori-Tanaka			
		$\bar{u}(-0.5h)$	$\bar{w}(0)$	$\bar{\sigma}_x(-0.34h)$	$\bar{\tau}_{xz}(0)$	$\bar{u}(-0.5h)$	$\bar{w}(0)$	$\bar{\sigma}_x(-0.34h)$	$\bar{\tau}_{xz}(0)$
1	5	2.1404	1.4098	-6.3537	0.74592	2.2873	1.5179	-6.4279	0.72877
	10	2.1157	1.3403	-6.3646	0.77474	2.2573	1.4329	-6.4410	0.75635
	20	2.1095	1.3229	-6.3673	0.78897	2.2497	1.4116	-6.4443	0.76999
4	5	2.5079	1.6646	-5.6811	0.75133	2.5770	1.7218	-5.3402	0.74292
	10	2.4729	1.5698	-5.6897	0.77841	2.5373	1.6136	-5.3496	0.77036
	20	2.4641	1.5461	-5.6918	0.79182	2.5273	1.5865	-5.3519	0.78396
10	5	2.6337	1.7578	-4.5413	0.75103	2.6646	1.7858	-4.4132	0.74719
	10	2.5934	1.6487	-4.5487	0.77891	2.6214	1.6684	-4.4210	0.77568
	20	2.5832	1.6214	-4.5506	0.79274	2.6104	1.6390	-4.4230	0.78983

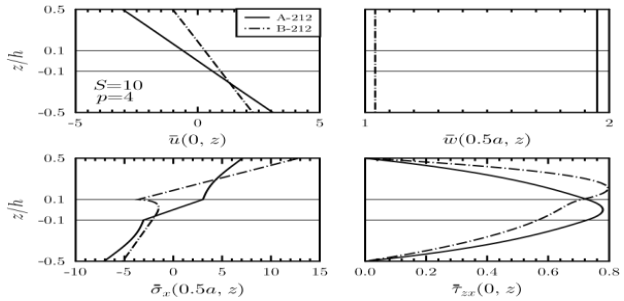


Figure 9: Through-thickness distributions under uniform loading using Mori-Tanaka model in FGM panels A and B with 2:1:2 thickness ratio

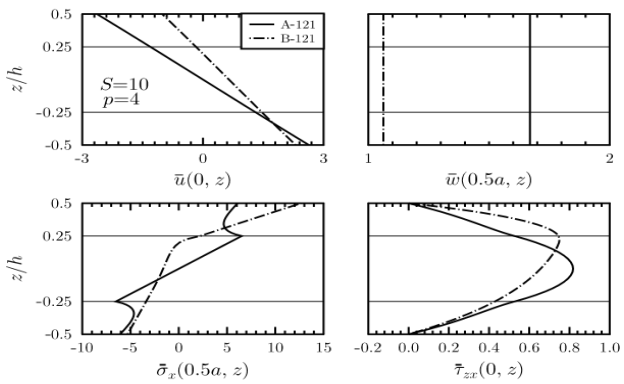


Figure 10: Through-thickness distributions under uniform loading using Mori-Tanaka model in FGM panels A and B with 1:2:1 thickness ratio

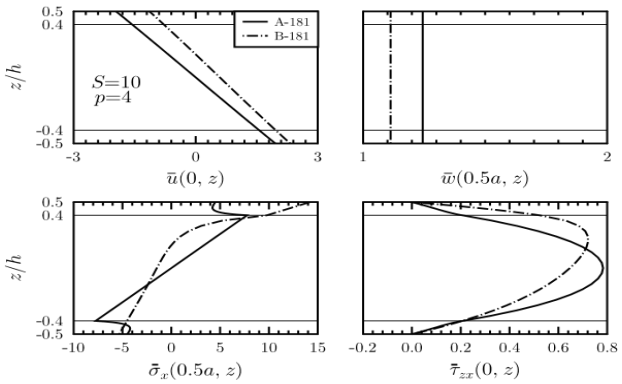


Figure 11: Through-thickness distributions under uniform loading using Mori-Tanaka model in FGM panels A and B with 1:8:1 thickness ratio

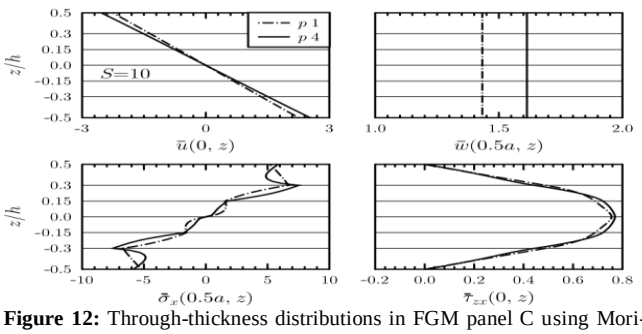


Figure 12: Through-thickness distributions in FGM panel C using Mori-Tanaka model under uniform loading

3.3. Free Vibration Analysis

The sandwich rectangular FGM panels A and B have three layers with thickness ratios for bottom skin to middle core to top skin as 2-1-2, 1-1-1, 1-2-1 and 1-8-1. The fundamental frequencies for this sandwich rectangular panels having above mentioned four thickness ratios with aspect ratio S = 5, 10 and 20 and power law index p = 1 and 4 are shown in Table 9. The natural frequency is found to decrease with increase of p. The sandwich rectangular FGM panel C has six layers. The fundamental frequencies for this sandwich rectangular panel for aspect ratio S = 5, 10 and 20, and power law index 1 and 4 are also shown in the same table. The natural frequency is found to decrease with increase of p.

4. Conclusion

A new analytical approach is developed and implemented for static and free vibration analysis of functionally graded material structures where the material laminate has continuous variation of material properties across thickness to get desired performance by predicting the displacements and stresses as local response and the natural frequencies as global response. The responses have been obtained for symmetric and nonsymmetric FGM laminates by adopting a layered approach. This analysis will facilitate the designers to choose suitable property variation, manufacture the laminate by additive manufacturing with a continuously varying composition of the constituents. Such materials and structures show a promise to the materials side of the fourth industrial revolution. The proposed analytical approach is simple, efficient as well as accurate and has a scope to be implemented in finite elements to handle more general geometry and boundary conditions.

References

[1] Koizumi M., FGM Activities in Japan, *Composites: Part B*, vol. 28B, pp. 1–4, 1997.

[2] Birman V., and Byrd L.W., Modelling and Analysis of Functionally Graded Materials and Structures, *Appl. Mech. Rev.*, vol. 60, pp. 195–216, 2007.

[3] Jha D.K., Kant T., and Singh R.K., A Critical Review of Recent Research on Functionally Graded Plates, *Compos. Struct.*, vol. 96, pp. 833–49, 2013.

[4] Swaminathan K., Naveenkumar D.T., Zenkour A.M., and Carrera E., Stress,Vibration and Buckling Analyses of FGM Plates-A State-of-The-Art Review, *Compos. Struct.*, vol. 120, pp. 10–31, 2015.

[5] Thai H., and Kim S., A Review of Theories for The Modeling and Analysis of Functionally Graded Plates and Shells, *Compos. Struct.*, vol. 128, pp. 70—86, 2015.

[6] Kashtalyan M., and Menshykova M., Three-Dimensional Elasticity Solution for Sandwich Panels With a Functionally Graded Core, *Compos. Struct.*, vol. 87, pp. 36–43, 2009.

[7] Li Q., Iu V.P., and Kou K.P., Three-Dimensional Vibration Analysis of Functionally Graded Material Sandwich Plates, *J. Sound Vib.*, vol. 311, pp. 498–515, 2008.

[8] Fantuzzi N., Brischetto S., Tornabene F., and Viola E., 2D and 3D Shell Models For The Free Vibration Investigation of Functionally Graded Cylindrical and Spherical Panels, *Compos. Struct.*, vol. 154, pp. 573–590, 2016.

[9] Wu C.P., and Li H.Y., The RMVT- and PVD-Based Finite Layer Methods For The Three-Dimensional Analysis of Multilayered Composite and FGM Plates, *Compos. Struct.*, vol. 92, pp. 2476–2496, 2010a.

[10] Nguyen T.K., Sab K., and Bonnet G., First-Order Shear Deformation Plate Models For Functionally Graded Materials, *Compos. Struct.*, vol. 83, pp. 25–36, 2008.

[11] Yang C., Jin G., Ye X., and Liu Z., A Modified Fourier-Ritz Solution For Vibration and Damping Analysis of Sandwich Plates With Viscoelastic and Functionally Graded Materials, *Int. J. Mech. Sci.*, vol. 106, pp. 1–18, 2016.

[12] Bernardo G.M.S., Damasio F.R., Silva T.A.N., and Loja M.A.R., A Study On The Structural Behaviour of FGM Plates Static and Free Vibrations Analyses, *Compos. Struct.*, vol. 136, pp. 124–138, 2016.

[13] Wu C.P., and Li H.Y., An RMVT-Based Third-Order Shear Deformation Theory of Multilayered Functionally Graded Material Plates, *Compos. Struct.*, vol. 92, pp. 2591–2605, 2010b.

[14] Zenkour A.M., A Comprehensive Analysis of Functionally Graded Sandwich Plates: Part 1-Deflection and Stresses, *Int. J. Solids Struct.*, vol. 42, pp. 5224–5242, 2005a.

[15] Zenkour A.M., A Comprehensive Analysis of Functionally Graded Sandwich Plates: Part 2-Buckling and Free Vibration, *Int. J. Solids Struct.*, vol. 42, pp. 5243–5258, 2005b.

[16] Mantari J.L., and Soares C. G., Five-Unknowns Generalized Hybrid-Type Quasi-3D HSDT For Advanced Composite Plates, *Appl. Math. Model.*, vol. 39, pp. 5598–5615, 2015.

[17] Mantari J.L., and Granados E.V., A Refined FSDT For The Static Analysis of Functionally Graded Sandwich Plates, *Thin Wall. Struct.*, vol. 90, pp. 150–158, 2015a.

[18] Zenkour A.M., Bending Analysis of Functionally Graded Sandwich Plates Using a Simple Four-Unknown Shear and Normal Deformations Theory, *J. Sand. Struct. Mater.*, vol. 15, pp. 629–656, 2013.

[19] Thai H.T., and Choi D.H., A Simple First-Order Shear Deformation Theory For The Bending and Free Vibration Analysis of Functionally Graded Plates, *Compos. Struct.*, vol. 101, pp. 332–340, 2013.

[20] Thai C.H., Kulasegaram S., Tran L.V., and Nguyen-Xuan H., Generalized Shear Deformation Theory For Functionally Graded Isotropic and Sandwich Plates Based on Isogeometric Approach, Comput. Struct., vol. 141, pp. 94–112, 2014a.

[21] Bennoun M., Houari M.S.A., and Tounsi A., A Novel Five-Variable Refined Plate Theory For Vibration Analysis of Functionally Graded Sandwich Plates, Mech. Adv. Mater. Struct., vol. 23, pp. 423–431, 2016.

[22] Nguyen V.H., Nguyen T.K., Thai H.T., and Vo T.P., A New Inverse Trigonometric Shear Deformation Theory For Isotropic and Functionally Graded Sandwich Plates, Composites: Part B, vol. 66, pp. 233–246, 2014.

[23] Mahi A., Bedia E.A.A., and Tounsi A., A New Hyperbolic Shear Deformation Theory For Bending and Free Vibration Analysis of Isotropic, Functionally Graded, Sandwich and Laminated Composite Plates, Appl. Math. Model., vol. 39, pp. 2489–2508, 2015.

[24] Liu M., Cheng Y., and Liu J., High-Order Free Vibration Analysis of Sandwich Plates With Both Functionally Graded Face Sheets and Functionally Graded Flexible Core, Composites: Part B, vol 72, pp. 97–107, 2015.

[25] Carrera E., Brischetto S., Cinefra M., and Soave M., Refined and Advanced Models For Multilayered Plates and Shells Embedding Functionally Ggraded Material Layers, Mech. Adv. Mater. Struct., vol. 17, pp. 603–621,2010.

[26] Neves A.M.A., Ferreira A.J.M., Carrera E., Cinefra M., Roque C.M.C., Jorge R.M.N., and Soares C.M.M., A Quasi-3D Hyperbolic Shear Deformation Theory For The Static and Free Vibration Analysis of Functionally Graded Plates, Compos. Struct., vol. 94, pp. 1814–1825, 2012a.

[27] Neves A.M.A., Ferreira A.J.M., Carrera E., Roque C.M.C., Cinefra M., Jorge R.M.N., and Soares C.M.M., A Quasi-3D Sinusoidal Shear Deformation Theory For The Static and Free Vibration Analysis of Functionally Graded Plates, Composites: Part B, vol. 43, pp. 711–725, 2012b.

[28] Neves A.M.A., Ferreira A.J.M., Carrera E., Cinefra M., Roque C.M.C., Jorge R.M.N., and Soares C.M.M., Static, Free Vibration and Buckling Analysis of Isotropic and Sandwich Functionally Graded Plates Using a Quasi-3D Higher-Order Shear Deformation Theory and a Meshless Technique, Composites: Part B, vol. 44, pp. 657–674, 2013.

[29] Alipour M.M., and Shariyat M., An Elasticity-Equilibrium-Based Zigzag Theory For Axisymmetric Bending and Stress Analysis of The Functionally Graded Circular Sandwich Plates, Using a Maclaurin-Type Series Solution, Eur. J. Mech. A/Solids, vol. 34, pp. 78–101, 2012.

[30] Alipour M.M., and Shariyat M., Analytical Zigzag-Elasticity Transient and Forced Dynamic Stress and Displacement Response Prediction of The Annular FGM Sandwich Plates, Compos. Struct., vol. 106, pp. 426–445, 2013.

[31] Voigt W., Uber die beziehung zwischen den beiden elastizit¨atskonstanten isotroper k¨orper. Wied Ann Phys 1889; 38: 573—87.

[32] Kapuria S., Patni M., and Yasin M.Y., A quadrilateral shallow shell element based on the third-order theory for functionally graded plates and shells and the inaccuracy of rule of mixtures, Eur. J. Mech. A/Solids 49 (2015) 268–282.

[33] Reddy J.N., Cheng Z.Q., Three-dimensional thermomechanical deformations of functionally graded rectangular plates, Eur. J. Mech. A/Solids 20 (2001) 841–855.

Table 9: Nondimensionalized natural frequencies for FGM panels A, B and C

p	*S*	ROM				Mori-Tanaka			
		2 – 1 – 2	1 – 1 – 1	1 – 2 – 1	1 – 8 – 1	2 – 1 – 2	1 – 1 – 1	1 – 2 – 1	1 – 8 – 1
Panel A									
1	5	24.808	25.132	25.727	27.396	24.107	24.459	25.135	27.098
	10	25.781	26.127	26.780	28.647	25.031	25.401	26.137	28.320
	20	26.048	26.400	27.070	28.995	25.284	25.659	26.412	28.659
4	5	23.109	23.329	24.009	26.477	22.914	23.103	23.771	26.334
	10	23.946	24.157	24.886	27.621	23.747	23.919	24.631	27.464
	20	24.174	24.383	25.125	27.937	23.974	24.141	24.865	27.776
Panel B									
1	5	31.383	31.747	32.418	34.059	30.878	30.890	31.059	31.429
	10	32.577	32.976	33.715	35.521	32.110	32.185	32.446	32.957
	20	32.905	33.314	34.072	35.926	32.450	32.543	32.832	33.385
4	5	30.854	30.811	30.856	30.820	30.673	30.556	30.504	30.041
	10	32.134	32.194	32.388	32.564	31.985	32.012	32.174	31.963
	20	32.488	32.580	32.819	33.061	32.349	32.419	32.649	32.519
Panel C									
ROM						Mori-Tanaka			
p	S = 5	S = 10	S = 20			p	S = 5	S = 10	S = 20
1	28.193	29.219	29.498			1	27.174	28.259	28.557
4	26.436	27.509	27.804			4	25.997	27.133	27.448